

Effects of Stress Path on Polyaxial Strengths of Maha Sarakham Salt

K. Artkhonghan* and K. Fuenkajorn

*Geomechanics Research Unit, Suranaree University of Technology
111 University Avenue, NakhonRatchasima 30000, Thailand*

* K.artkhonghan@gmail.com

Abstract

The objectives of this study are to determine strength and stiffness of rock salt under different stress paths in the laboratory and to evaluate the predictability of the existing failure criteria and their parameters. The effects of stress paths have been studied through the triaxial compression and triaxial extension tests. The prepared specimens are rock salt from the Maha Sarakham formation at depths ranging from 150 to 300 m. The specimens have the rectangular blocks with normal dimensions of $4.4 \times 4.4 \times 8.8$ cm³. A true triaxial loading device is developed for this study. Four different stress paths have been implemented: (I) σ_1 increases while σ_2 and σ_3 are equally maintained constant; (II) σ_1 increases while σ_2 and σ_3 are simultaneously decreases; (III) σ_1 and σ_2 equally increase while σ_3 are maintained constant; and (IV) σ_1 and σ_2 equally increase while σ_3 decreases. For the stress paths (I) and (III), the mean stress (σ_m) is increased during testing (conventional method) and for the other two, the mean stress is maintained constant (constant mean stress method). The results indicate that the strengths obtained for the triaxial extension is lower than those of the triaxial compression. The strengths of the constant mean stress method are lower than those of the conventional method. The elastic modulus and Poisson's ratio tend to be independent of the stress path. The modified Wiebols and Cook criterion can well predict the triaxial strengths under different stress paths with the coefficient of correlations of 0.91 for path (I) and (III) and 0.89 for path (II) and (IV).

Keywords: Stress path, Mean stress, Strength, Triaxial, Rock Salt.

1. Introduction

The reliable strength estimation of a rock salt is necessary to develop safe and economical designs for solution mining, compressed-air energy storage and underground salt mining. Rock salt is an inhomogeneous and anisotropic material with complex behavior. The effects of confining pressures at great depths on the mechanical properties of rocks are commonly simulated in a laboratory by performing triaxial compression testing. A significant limitation of these conventional methods is that the mean stress is not constant during the test. The actual in-situ rock is normally subjected to an anisotropic stress state where the maximum, intermediate and minimum principal stresses are different ($\sigma_1 \neq \sigma_2 \neq \sigma_3$) and mean stress of this condition is always constant. It has been commonly found that compressive strengths obtained from conventional polyaxial load frame or true triaxial load

frame can represent the actual in-situ strength where the rock is subjected to an anisotropic stress state.

Researchers from the field of material sciences believe that rock salt behaviour shows many similarities with that of various metals and ceramics (Chokski and Langdon, 1991). However, because alkali halides are ionic materials, there are some important differences in their behavior. Aubertin et al. (1993, 1999) conclude that the rock salt behavior should be brittle-to ductile materials or elastic-plastic behavior. This also agrees with the findings by Fuenkajorn and Daemen (1988)

The strength and deformation behavior of rock material are dependent on the loading path, which have been widely investigated in the past decades to understand and explore the fracture mechanism of various rock engineering (such deep underground rock engineering, and tunnel rock engineering, etc.) under different loading paths (Crouch, 1972; Yao et al., 1980; Xu and Geng, 1986; Lee et al., 1999; Wang et al., 2008; Yang et al., 2011; Yang et al., 2012). In the previous studies, two kinds of loading paths, i.e. conventional triaxial compression and confining pressure reduction, are often adopted to analyze the strength and deformation behavior of all kinds of rock material. On the influence of the loading path on the strength of rock, there are two kinds of contradictory opinions. One opinion regarded that the strength of the rock was independent of the stress path by carrying out triaxial compression experiment for granite and norite (Swanson and Brown, 1971). Another opinion regarded that the loading path had a significant influence on the loading path.

The objectives of this study are to invent a triaxial rock testing device, to determine the compressive strength of the rocksalt subjected to triaxial stress states, to investigate the influence of the intermediate stress on rock failure, and to develop three dimensional failure criterion of the rocks that can be readily applied in the design and the stability analysis of geologic structures.

2. True triaxial compression test

The polyaxial compression tests are performed to investigate the effects of stress paths on the compressive strengths and the deformations of rock salt. The test equipment for the polyaxial compression tests is the true triaxial loading device. Figure 1 shows the isometric drawing of the true triaxial loading device (on the right side) and the picture of this device during the tests. This device is developed to test the rock specimens with soft to medium strengths under biaxial and polyaxial stress states. During the test each set of the three load frames will apply independent loads to provide different principal stresses ($\sigma_1 \neq \sigma_2 \neq \sigma_3$) on to the rock specimens. This loading device can accommodate the cubic or rectangular specimens of different sizes by adjusting the distances between the opposite steel loading platens. For this study, the rock specimens have the rectangular block with normal size of $4.4 \times 4.4 \times 8.8 \text{ cm}^3$, placed around the center of device. Four different stress paths have been implemented: (I) σ_1 increases while σ_2 and σ_3 are equally maintained constant; (II) σ_1 increases while σ_2 and σ_3 are simultaneously decreases; (III) σ_1 and σ_2 equally increase while σ_3 are maintained constant; and (IV) σ_1 and σ_2 equally increase while σ_3 decreases. Table 1 summarizes the testing specification for each stress paths.

For all tests, neoprene sheets are used to minimize the friction at all interfaces between the loading platens and the specimen surfaces. The measured deformations are used to determine the strains along the principal axes during loading. The failure stresses are recorded and modes of failure are examined.

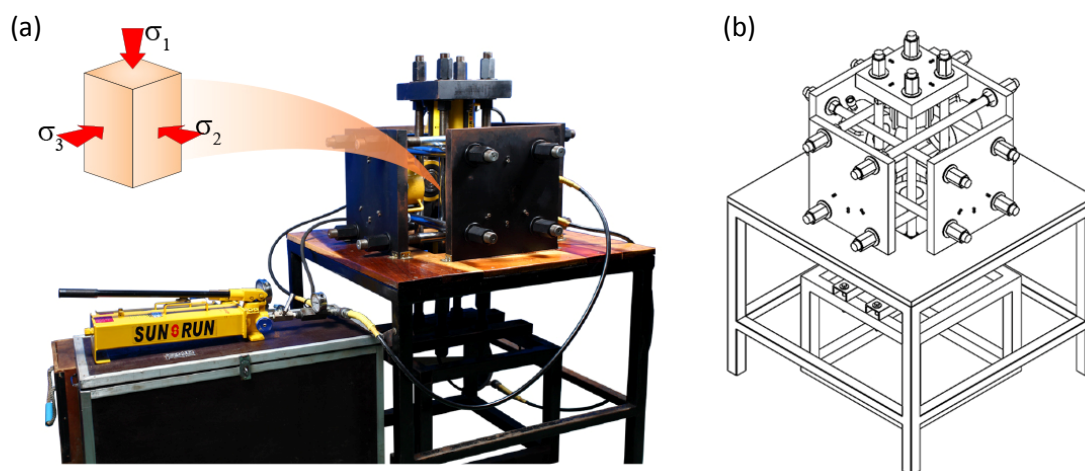


Fig. 1.(a) Typical picture of true triaxial loading device during the true triaxial test. (b) General isometric drawing of the true triaxial loading device.

Table 1. Summary of the testing specifications for each stress paths.

Test condition	Path	Loading	Number of Samples	Applied stresses (MPa)
Triaxial compression	I	Conventional (Constant σ_3)	10	$\sigma_3 = 1, 3, 5, 7, 10, 12, 20, 28, 38, 45$
	II	Constant mean stress (Constant σ_m)	10	$\sigma_m = 15, 17, 20, 22, 26, 30, 35, 43, 57, 80$
Triaxial extension	III	Conventional (Constant σ_3)	8	$\sigma_3 = 0, 0.5, 1, 3, 5, 6.5, 10, 12$
	IV	Constant mean stress (Constant σ_m)	8	$\sigma_m = 26, 35, 40, 43, 52, 60, 70, 80$

3. Test Results

Table 2 summarizes the strength results from true triaxial tests for different stress paths for each rock sample. For triaxial compression tests, stress path (I) (constant σ_3) provides higher rock strengths than does stress path (II) (constant σ_m). Based on the Table 2 ($\sigma_2 = \sigma_3 \approx 3$ MPa), sample has failure stress at 45.1 under stress path (I) and 42.7 MPa under path (II). For triaxial extension tests, stress path (III) (constant σ_3) yields higher strengths, compared to the stress path (IV) (constant σ_m). From Table 2 ($\sigma_3 \approx$

5 MPa), failure stress is equal to 79.6 MPa under stress path (III) and 76.0 MPa under stress path (IV). The triaxial extension test gives higher strengths than the triaxial compression test. For example, under the condition of constant σ_3 , triaxial extension stress path (III) yields higher strengths of specimens than triaxial compression stress path (I). Figure 2 compares the strength results.

Table 2. Strength results.

Triaxial compression				Triaxial extension			
Stress path (I) (constant σ_3)		Stress path (II) (constant σ_m)		Stress path (III) (constant σ_3)		Stress path (IV) (constant σ_m)	
$\sigma_2 = \sigma_3$ (MPa)	σ_1 (MPa)	$\sigma_2 = \sigma_3$ (MPa)	σ_1 (MPa)	σ_3 (MPa)	$\sigma_1 = \sigma_2$ (MPa)	σ_3 (MPa)	$\sigma_1 = \sigma_2$ (MPa)
1.0	26.5	1.0	25.6	0.0	35.1	0.5	39.5
3.0	41.5	3.1	42.7	0.5	40.4	1.1	47.2
5.0	58.6	4.3	55.1	1	49.3	2.0	52.5
7.0	66.3	7.0	65.0	3	64.9	3.3	60.7
10.0	79.6	10.8	76.5	5	79.6	5.1	72.6
12.0	81.8	11.5	79.4	6.5	85.5	7.3	80.1
20.0	106.4	19.9	91.2	10	98.1	9.9	85.7
28.0	119.7	29.1	109.9	12	107.9	11.7	90.5
38.0	132.5	40.5	130.0	N/A	N/A	N/A	N/A
45.0	145.5	46.7	143.2	N/A	N/A	N/A	N/A

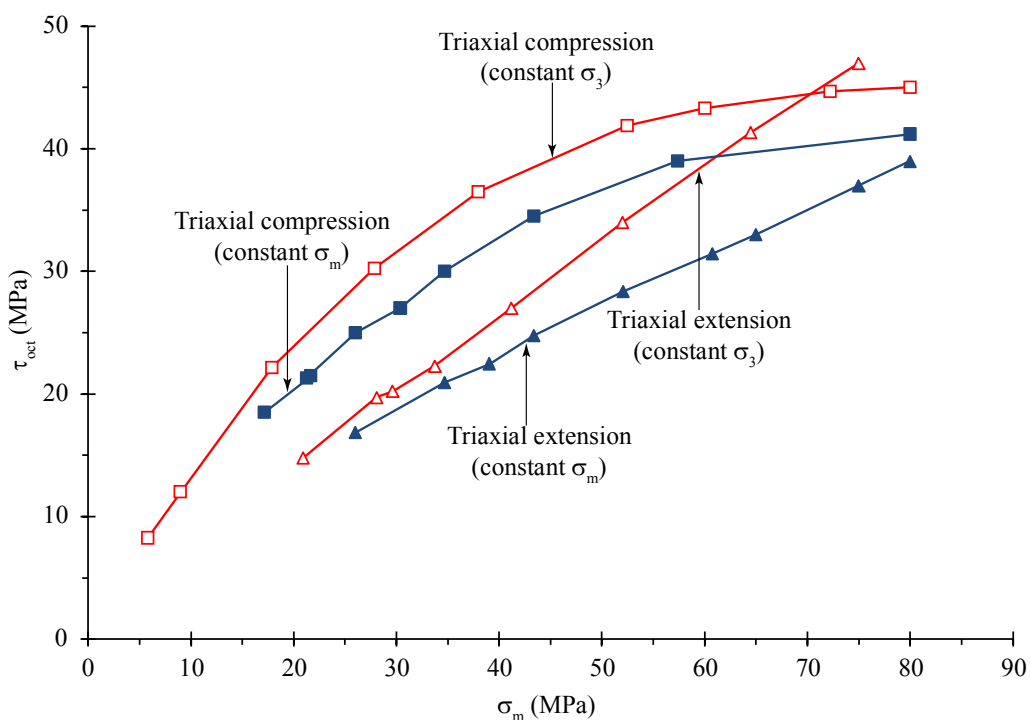


Fig. 2. Octahedral shear stresses (τ_{oct}) as a function mean stress (σ_m).

4. Modified Wiebols and Cook

The test results are compared with the modified Wiebols and Cook. This criteria selected because the Coulomb criterion has been widely used in actual field applications while the modified Wiebols and Cook criterion has been claimed by many researchers to be one of the best representations of rock strengths under confinement. The modified Wiebols and Cook criterion is proposed by Zhou (1994). The criterion is originally developed by Wiebols and Cook (1968) based on the additional energy stored around Griffith cracks due to the sliding of crack surfaces over each other. The modified version by Colmenares and Zoback (2002) defines $J_2^{1/2}$ at failure in terms of J_1 as:

$$J_2^{1/2} = A + BJ_1 + C J_1^2 \quad (1)$$

$$J_2^{1/2} = [1/6 ((\sigma_1 - \sigma_2)^2 + (\sigma_1 - \sigma_3)^2 + (\sigma_2 - \sigma_3)^2)]^{1/2} = (3/2)^{1/2} \tau_{oct} \quad (2)$$

$$J_1 = (1/3) \times (\sigma_1 + \sigma_2 + \sigma_3) \quad (3)$$

$$\tau_{oct} = 1/3 [(\sigma_1 - \sigma_2)^2 + (\sigma_2 - \sigma_3)^2 + (\sigma_3 - \sigma_1)^2]^{1/2} \quad (4)$$

where J_1 is the mean effective confining stress and; where τ_{oct} is the octahedral shear stress.

The constants A, B and C depend on rock materials and the minimum principal stresses (σ_3). They can be determined under the conditions where $\sigma_2 = \sigma_3$, as follows (Colmenares and Zoback, 2002):

$$A = C_0/3^{1/2} - BC_0/3 - CC_0^2/9 \quad (5)$$

$$B = 3^{1/2} (q-1)/(q+2) - C/3(2C_0 + (q+2)\sigma_3) \quad (6)$$

$$C = [27^{1/2} / (2C_1 + (q-1)\sigma_3 - C_0)] \times \\ [[(C_1 + (q-1)\sigma_3 - C_0)/(2C_1 + (2q+1)\sigma_3 - C_0)] - [(q-1)/(q+2)]] \quad (7)$$

where $C_1 = (1 + 0.6\mu) C_0$;

C_0 = uniaxial; compressive strength of the rock;

$\mu = \tan \phi$;

$q = [(\mu^2 + 1)^{1/2} + \mu]^2 = \tan^2 (\pi/4 + \phi/2)$;

μ = coefficient of internal friction of the material;

ϕ = angle of internal friction.

For the triaxial tests of four different stress paths, the strength calculations in terms of τ_{oct} and σ_m (or J_1) and the numerical values A, B and C are given in Tables 3. The relationship between octahedral shear stress as a function of mean stress is shown in Figure 3.

Table 3. Strength calculation and numerical values.

Path	σ_1 (MPa)	σ_2 (MPa)	σ_3 (MPa)	σ_m (MPa)	τ_{oct} (MPa)	Numerical values		
						A	B	C
Stress path (I) Triaxial compression	26.5	1.0	1.0	9.5	12.0			
	41.5	3.0	3.0	15.8	18.1			
	58.6	5.0	5.0	22.8	25.2			
	66.3	7.0	7.0	26.7	27.9			
	79.6	10.0	10.0	33.2	32.8	1.698	1.711	-0.015
	81.8	12.0	12.0	35.2	32.9			
	119.7	28.0	28.0	58.5	43.2			
	132.5	38.0	38.0	69.5	44.5			
	145.5	45.0	45.0	78.5	47.3			
Stress path (II) Triaxial compression	25.6	1.0	1.0	9.2	11.6			
	42.7	3.1	3.1	16.3	18.7			
	55.1	4.3	4.3	21.2	23.9			
	65.0	7.0	7.0	26.3	27.3			
	76.5	10.8	10.8	32.7	30.9	2.115	1.746	-0.033
	79.4	11.5	11.5	34.1	32.0			
	109.9	29.1	29.1	56.0	38.1			
	130.0	40.5	40.5	70.3	42.2			
	143.2	46.7	46.7	78.8	45.5			
Stress path (III) Triaxial extension	35.1	35.1	0.0	23.4	16.5			
	40.4	40.4	0.5	27.1	18.8			
	49.3	49.3	1	33.2	22.7			
	64.9	64.9	3	44.2	29.1	1.698	1.711	-0.015
	79.6	79.6	5	54.7	35.1			
	85.5	85.5	6.5	59.1	37.2			
	98.1	98.1	10	68.7	41.5			
	107.9	107.9	12	75.9	45.2			
Stress path (IV) Triaxial extension	39.5	39.5	0.5	26.5	18.3			
	47.2	47.2	1.1	31.8	21.7			
	52.5	52.5	2.0	35.6	23.8			
	60.7	60.7	3.3	41.5	27.0	2.115	1.746	-0.033
	72.6	72.6	5.1	50.1	31.8			
	80.1	80.1	7.3	55.8	34.3			
	85.7	85.7	9.9	60.4	35.7			
	90.5	90.5	11.7	64.2	37.1			

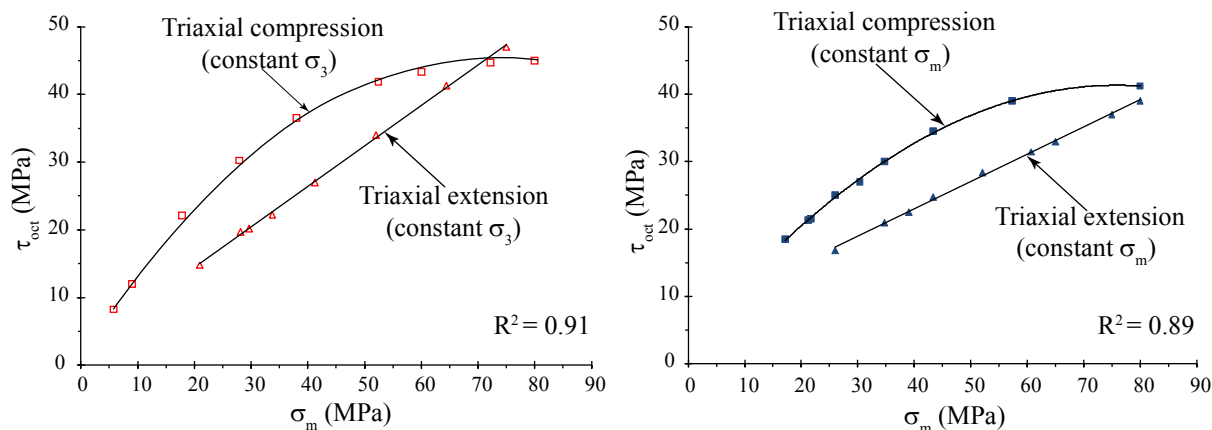


Fig.3. Test results fitted by the modified Wiebols& Cook criterion.

5. Elastic Parameters

The elastic parameters are calculated for the three-dimensional principal stress-strain relations. The calculations of elastic parameters are made at 30-40% of the maximum principal stresses. An attempt is made to calculate the elastic moduli along the three loading directions. It is assumed here that the Poisson's ratio (ν) of each rock specimen is the same for all principal planes. The elastic moduli along the major, intermediate and minor principal directions can be calculated by (Jaeger et al., 2007):

$$\epsilon_1 = \sigma_1 / E_1 - \nu (\sigma_2 / E_2 + \sigma_3 / E_3) \tag{8}$$

$$\epsilon_2 = \sigma_2 / E_2 - \nu (\sigma_1 / E_1 + \sigma_3 / E_3) \tag{9}$$

$$\epsilon_3 = \sigma_3 / E_3 - \nu (\sigma_1 / E_1 + \sigma_2 / E_2) \tag{10}$$

Where ϵ_1 , ϵ_2 and ϵ_3 are the major, intermediate and minor principal strains, and E_1 , E_2 and E_3 are the elastic moduli along the major, intermediate and minor directions. The calculation results are shown in Figure4 which suggests that the elastic moduli along the principal directions are similar. The discrepancies shown in Figure4 are probably due to the intrinsic variability of each rock specimens. Table 4 summarizes the elastic modulus and Poisson's ratio.

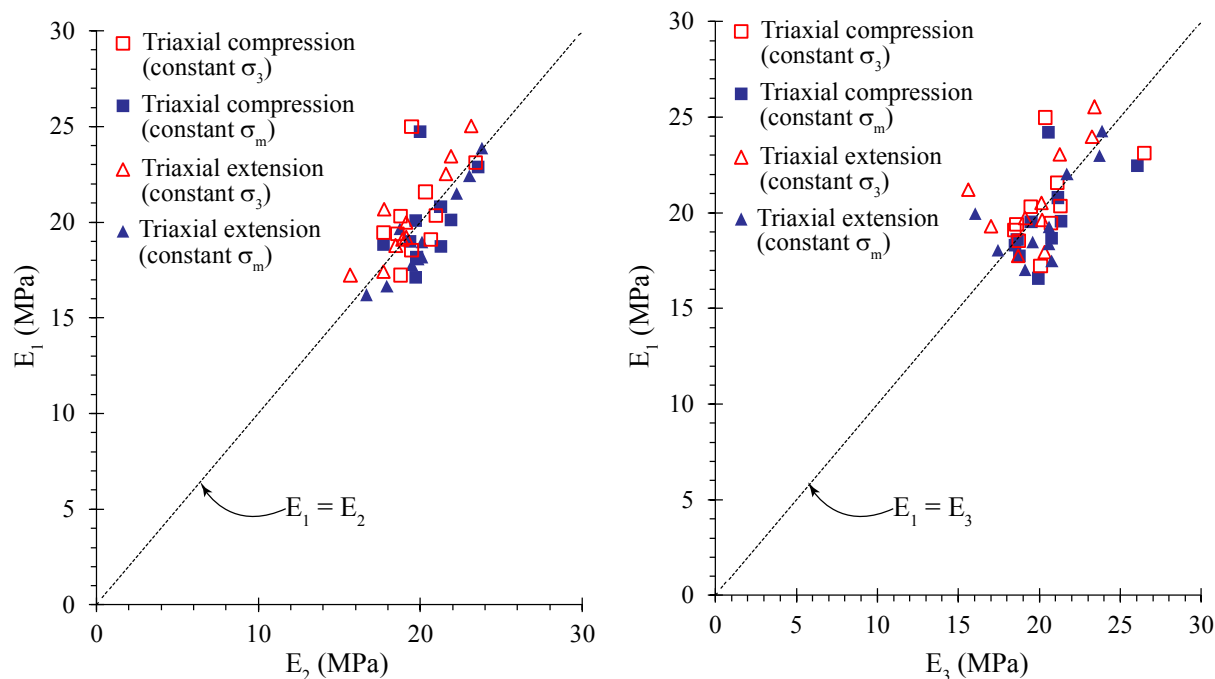


Fig. 4. Elastic modulus calculated along the major principal axes as a function of intermediate and minor principal axes.

Table 4. Summary of the elastic modulus and Poisson's ratio.

Stress path	Mean elastic modulus (MPa)	Poisson's ratio	Range of σ_3 (MPa)
Path (I) Triaxial compression (constant σ_3)	20.4 ± 2.3	0.40 ± 0.03	0 – 12.0
Path (II) Triaxial compression (constant σ_m)	19.36 ± 0.19	0.38 ± 0.02	8.1 – 27.0
Path (III) Triaxial extension (constant σ_3)	22.78 ± 1.86	0.40 ± 0.01	0 – 12.0
Path (IV) Triaxial extension (constant σ_m)	20.53 ± 1.43	0.39 ± 0.03	5.0 – 27.0

6. Discussions and Conclusions

The average standard deviation of the rock salt elastic modulus is 10.96%. This standard deviation suggests that the fabricated rock testing device performs reasonably well. The assumption of using the Poisson's ratio of 0.4 to determine the elastic moduli for all principal planes should be considered as a reasonable assumption. These assumed ratios are the average values which are calculated from the results of the tests by reasonable good testing device.

The discrepancies of the test results may be partly derived from some characteristics of the selected rock types used as specimens. Rock salt elements are chemical materials. Therefore, it may be a cause of the high standard deviation of its mean elastic modulus value. Normally, the elastic modulus

in the direction parallel to the bedding planes is greater than that normal to the bedding. The Poisson's ratio on the plane parallel to the bedding is lower than the ratio on the plane normal to it. Under similar condition, the stress paths with σ_3 is constant (stress path (I) and (III)) usually yield higher value of elastic modulus for different rock specimens than the one with σ_m is constant {stress path (II) and (IV)}, which results from the influence of σ_2 and σ_3 .

The sizes of the applied loading areas partly affect the outcome of the test results. Smaller areas may cause higher degree of intrinsic variability of rock specimens, providing more standard deviation of the elastic modulus values. Therefore, the selection of the appropriate nominal sizes of specimens may enhance more consistencies of the experimental results.

The triaxial compression testing with σ_3 is constant yields higher strength values than those of triaxial extension test. This implies that if the conventional triaxial test results are applied in the stability analysis and design of in-situ rock that are subject to triaxial extension condition, the result of such analyzes may not be conservative. Testing under constant σ_m is therefore desirable and should provide the results close to the in-situ condition, particularly for the underground structures (tunnels and mine openings).

Acknowledgements

This study is funded by Suranaree University of Technology and by the Higher Education Promotion and National Research University of Thailand. Per-mission to publish this paper is gratefully acknowledged.

References

- Aubertin, M., Gill, D. E. and Ladanyi, B., 1993, Modelling the transient inelastic flow of rock salt, *Proceedings of Seventh Symposium on Salt*, Kyoto, Japan, April 1992, Elsevier Science Publishers, Amsterdam, Vol. I, pp. 93-104.
- Aubertin, M., Julien, M. R., Servant, S. and Gill, D. E., 1999, A rate-dependent model for the ductile behavior of salt rocks, *Canadian Geotechnical Journal*, Vol. 36, No.4, Canada, pp. 660-674
- Chokski, A. H. and Langdon, T. G., 1991, *Characteristics of creep deformation in ceramics*, Materials Science and Technology, Vol. 7, pp. 577-584.
- Crouch, S.L., 1972. A note on post-failure stress-strain path dependence in norite. *International Journal of Rock Mechanics and Mining Sciences* 9 (2), 197-204.
- Fuenkajorn, K. and Daemen, J. J. K. (1988). *Boreholes closure in salt. Technical Report Prepared for The U.S. Nuclear Regulatory Commission*. Report No. NUREG/CR-5243 RW. University of Arizona.
- Lee, D.H., Juang, C.H., Chen, J.W., et al., 1999. Stress paths and mechanical behavior of a sandstone in hollow cylinder tests. *International Journal of Rock Mechanics and Mining Sciences* 36, 857-870.

- Swanson, R.S., Brown, W.S., 1971. An observation of loading path independence of fracture in rock. *International Journal of Rock Mechanics and Mining Sciences* 8 (3), 277–281.
- Wang, B., Zhu, J.B., Wu, A.Q., et al., 2008. Experimental study on mechanical properties of Jinping marble under loading and unloading stress paths. *Chinese Journal of Rock Mechanics and Engineering* 27 (10), 2138–2145.
- Yang, S.Q., Jing, H.W., Li, Y.S., Han, L.J., 2011. *Experimental investigation on mechanical behavior of coarse marble under six different loading paths*. *Experimental Mechanics* 51 (3), 315–334.
- Yang, S.Q., Jing, H.W., Wang, S.Y., 2012. Experimental investigation on the strength, deformability, failure behavior and acoustic emission locations of red sandstone under triaxial compression. *Rock Mechanics and Rock Engineering* 45 (4), 583–606.
- Yao, X.X., Geng, N.G., Chen, Y., 1980. *The effect of stress path on brittleness and ductility of rocks*. *Acta Geophysica Sinica* 23 (3), 312–319.